Chlorostannate(II) Ionic Liquids: Speciation, Lewis Acidity, and Oxidative Stability

Matthew Currie,[†] Julien Estager,[†,‡] Peter Licence,*[§] Shuang Men,[§] Peter Nockemann,[†] Kenneth R. Seddon,[†] Małgorzata Swadźba-Kwaśny,*[†] and Cécile Terrade[†]

[†]QUILL, The Queen's University of Belfast, Belfast BT9 5AG, United Kingdom
[§]School of Chemistry, The University of Nottingham, Nottingham NG7 2RD, United Kingdom

Ⓢ Supporting Information

ABSTRACT: The anionic speciation of chlorostannate(II) ionic liquids, prepared by mixing 1-alkyl-3-methylimidazolium chloride and tin(II) chloride in various molar ratios, χ_{SnCl_2}, was investigated in both solid and liquid states. The room temperature ionic liquids were investigated by ^{119}Sn NMR spectroscopy, X-ray photoelectron spectroscopy, and viscometry. Crystalline samples were studied using Raman spectroscopy, single-crystal X-ray crystallography, and differential scanning calorimetry. Both liquid and solid systems (crystallized from the melt) contained $[SnCl_3]^-$ in equilibrium with Cl^- when $\chi_{SnCl_2} < 0.50$, $[SnCl_3]^-$ in equilibrium with $[Sn_2Cl_5]^-$ when $\chi_{SnCl_2} > 0.50$, and only $[SnCl_3]^-$ when $\chi_{SnCl_2} = 0.50$.

Tin(II) chloride was found to precipitate when $\chi_{SnCl_2} > 0.63$. No evidence was detected for the existence of $[SnCl_4]^{2-}$ across the entire range of χ_{SnCl_2}, although such anions have been reported in the literature for chlorostannate(II) organic salts crystallized from organic solvents. Furthermore, the Lewis acidity of the chlorostannate(II)-based systems, expressed by their Gutmann acceptor number, has been determined as a function of the composition, χ_{SnCl_2}, to reveal Lewis acidity for $\chi_{SnCl_2} > 0.50$ samples comparable to the analogous systems based on zinc(II). A change of the Lewis basicity of the anion was estimated using ^1H NMR spectroscopy, by comparison of the measured chemical shifts of the C-2 hydrogen in the imidazolium ring. Finally, compositions containing free chloride anions ($\chi_{SnCl_2} < 0.50$) were found to oxidize slowly in air to form a chlorostannate(IV) ionic liquid containing the $[SnCl_6]^{2-}$ anion.
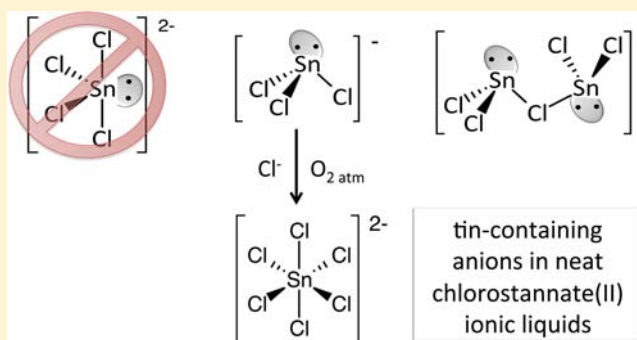
■ INTRODUCTION

Among numerous "families" of ionic liquids, those incorporating chlorometallate anions remain of the highest importance for industry. Chloroaluminate(III) systems have been used in key industrial processes, including the IFP Difasol process, the hydrosilylation of carbon double bounds by Degussa, and the alkylation of aromatics by BP.[1] The catalytic properties (in particular due to their Lewis acidity) of other chlorometallate ionic liquids have also been tested in a wide range of organic reactions,[2] including aryl cross-coupling with chloroferrates-(III),[3] oligomerization of alkenes using chlorogallate(III) systems,[4] and alkylation of phenols using chloroindate(III) systems.[5] Despite their inherent applicability, most chlorometallate ionic liquids pose serious operational issues: systems based on aluminum(III) and gallium(III) are sensitive toward moisture, while those incorporating gallium(III) or indium(III) are expensive.

Chlorostannates(II), on the other hand, are relatively inexpensive and stable in the presence of moisture.[6] In 1972, Parshall used tetraalkylammonium chlorostannate(II) salts, which are low melting, as solvents for different palladium-

catalyzed reactions of alkenes, such as hydrogenations, isomerizations, hydroformylations, and carboalkylations.[6] Wasserscheid and Waffenschmidt employed a similar bimetallic system, composed of tin and palladium, albeit liquid at ambient conditions, for hydroformylation.[7] More recently, chlorostannate(II) ionic liquids have been used in the synthesis of dimethylcarbonate from urea and methanol[8] and in the ring-opening polymerization of ethylene carbonate.[9] They have also been tested in a continuous process; for example, Wasserscheid and co-workers described the desulfurization of heptane over an equimolar mixture of 1-dodecyl-3-methylimidazolium chloride and tin(II) chloride, supported on alumina.[10]

Chlorometallate ionic liquids are typically synthesized via direct mixing of a metal chloride with an organic chloride salt (e.g., 1-alkyl-3-methylimidazolium chloride, $[C_nmim]Cl$, where $n = 1-18$). The catalytic properties of chlorometallate ionic liquids, and their Lewis acidity, are dependent on both the nature of the metal incorporated into the ionic liquid and the

ratio of metal chloride to organic chloride salt.[11] Hence, by tuning the ratio of metal chloride to organic chloride salt (expressed as the mole fraction of metal chloride, χ_{MClx}), it is possible to modify the coordination chemistry of chlorometallate anions and thus the Lewis acidity of the ionic liquid.

Anionic speciation has been determined unambiguously for many chlorometallate systems, such as chloroaluminate(III),[12] chloroindate(III),[13] chlorogallate(III),[14] or chlorozincate(II)[15] ionic liquids. It has also been demonstrated that speciation is directly related to the Lewis acidity, expressed as a Gutmann acceptor number (AN).[11,15,16]

In the present paper, we investigate quantification of the Lewis acidity of chlorostannate(II) ionic liquids via measurement of their acceptor properties and correlation of the observed changes in the acidity to speciation. Furthermore, anionic speciations of the chlorostannate(II) systems in solid and liquid phases are compared.

■ MATERIALS AND METHODS

Triethylphosphine oxide (tepo) was purchased from Sigma-Aldrich and opened in a dinitrogen-filled glovebox (MBraun LabMaster dp; <0.1 ppm O_2 and H_2O). Tin(II) chloride (98%) was also purchased from Sigma-Aldrich. 1-Ethyl-3-methylimidazolium chloride[17] and 1-octyl-3-methylimidazolium chloride[11] were prepared as described elsewhere, dried under a high vacuum (75 °C, 7 days, 10^{-3} mbar), and stored in a glovebox.

Synthetic Methods. *Preparation of Anhydrous Tin(II) Chloride.* In a typical procedure,[18] tin(II) chloride (50 g) was dissolved in a mixture of absolute ethanol (75 g) and 1,2-dichloroethane (425 g). Subsequently, the volume of the solution was reduced by ca. 50% by atmospheric distillation (100 °C). The remaining mixture, with partially precipitated tin(II) chloride, was stored overnight in the refrigerator to enhance further crystallization. The crystalline white powder was collected by filtration under reduced pressure, dried under a high vacuum (100 °C, 2 h), and immediately transferred into a glovebox, where it was stored. A typical yield was ca. 90%.

Synthesis of [$C_n$mim]Cl–$SnCl_2$ (n = 2 or 8) Systems. A range of compositions (0.25 ≤ χ_{SnCl_2} ≤ 0.75) of chlorostannate(II) ionic liquids based on 1-octyl-3-methylimidazolium or 1-ethyl-3-methylimidazolium cations were prepared. In a glovebox, an appropriate amount of [$C_n$mim]Cl (Table 1) was weighed into a sample vial (10 cm^{-3}) equipped with a poly(tetrafluoroethylene) (PTFE)-coated stirring bar. With the vial on the balance (±0.0002 g), an appropriate amount of tin(II) chloride was added to achieve the desired ratio of the reactants. Subsequently, the sample vial was closed with a cap, placed in a

Table 1. Mass of the Reactants (m/g) for the Synthesis of [$C_n$mim]Cl–$SnCl_2$ (n = 2 or 8) Systems

	n = 2			n = 8	
χ_{SnCl_2}	$m_{[C_2mim]Cl}$	m_{SnCl_2}	χ_{SnCl_2}	$m_{[C_8mim]Cl}$	m_{SnCl_2}
0.10	2.6253	0.3721	0.10	7.1746	0.6648
0.20	2.2466	0.7259	0.20	6.6144	1.3587
0.25	2.0789	0.8960	0.25	6.2783	1.7195
0.30	1.9239	1.0701	0.30	5.8945	2.0767
0.33	1.8326	1.1580	0.33	5.6284	2.2776
0.40	1.6062	1.3792	0.40	5.1513	2.8215
0.45	1.4575	1.5356	0.45	4.9075	3.2991
0.50	1.3082	1.6521	0.50	4.3052	3.5376
0.55	1.1665	1.8335	0.55	3.9915	4.0087
0.60	1.0204	1.9800	0.63	3.3734	4.8120
0.63	0.9265	2.0645	0.60	3.5275	4.3975
0.67	0.8274	1.9314	0.67	2.9689	4.9721
0.75	0.6123	2.3764	0.75	2.2944	5.6568

multiwell heater–stirrer (80 °C), and stirred vigorously overnight. The samples were stored in a glovebox prior to study.

Analytical Methods. *^{31}P NMR Spectroscopic Experiments for AN Calculations for [C_8mim]Cl–$SnCl_2$.* In a glovebox, a sample (1.00 g) of each 1-octyl-3-methylimidazolium chlorostannate(II) ionic liquid was weighed into a sample vial (10 cm^3) equipped with a PTFE-coated magnetic stirring bar. The vial was left on the balance, and tepo was added (ca. 5 mol % per mol of [C_8mim]$^+$ cation; an accurate mass of tepo was recorded and used for calculations). Then, solutions containing 10 and 15 mol % of tepo per 1 mol of [C_8mim]$^+$ cation were prepared for all compositions.

Subsequently, the sample vial was closed with a plastic cap and the mixture was stirred overnight at 55 °C to ensure full dissolution. The resulting liquid was loaded into an NMR tube (5 mm, borosilicate glass) containing a sealed capillary with dimethyl-d_6 sulfoxide to maintain a suitable lock signal. The tube was closed with a standard cap, sealed with parafilm, and removed from the glovebox immediately prior to measurement.

^{31}P NMR spectra were acquired at 161.98 MHz, using a Bruker Avance III 400 spectrometer. Phosphoric(V) acid, 85% solution in water, was used as the external reference. All samples were measured at 27 °C. ^{31}P NMR spectra of three solutions of tepo in hexane (ca. 5, 10, and 15 mol %) were also recorded, and the ^{31}P NMR chemical shift for the infinite dilution of tepo in hexane, $\delta_{inf\ hex}$, was determined by extrapolation. All other chemical shifts were reported relative to this value.[19]

^1H and ^{119}Sn NMR Spectroscopy of [C_8mim]Cl–$SnCl_2$. In a glovebox, neat ionic liquids were loaded into NMR tubes (5 mm, borosilicate glass) containing sealed capillaries with dimethyl-d_6 sulfoxide (an external lock). The tubes were closed with a standard cap, sealed with parafilm, and removed from the glovebox immediately prior to measurement.

For ^1H NMR nuclei, the spectra were recorded at 300.0 MHz, 27 °C, using a Bruker DRX 300 spectrometer and for ^{119}Sn NMR nuclei at 186.48 MHz, 80 °C, using a Bruker DRX 500 spectrometer. Neat tin(IV) chloride was used as an external reference ($\delta = -150.0$ ppm).

Viscometry of [C_8mim]Cl–$SnCl_2$. Measurements were carried out using a Bohlin Gemini cone-and-plate viscometer and rheometer with a Bohlin Instruments Peltier temperature control and a stainless steel 4/40 spindle. The viscosity was measured within the temperature range of 20–85 °C, in 5 °C increments, with two measurements taken at each temperature. Tested samples were loaded into syringes in the glovebox and transferred immediately to the apparatus.

X-ray Photoelectron Spectroscopy (XPS).[13c,20–23] Samples were prepared by placing a small drop (ca. 20 mg) of the ionic liquid into the depression of a stainless steel sample stub (designed for powders) or on a standard stainless steel multisample bar (both Kratos designs). The ionic liquid samples were cast into thin films ex situ (approximate thicknesses of 0.5–1 mm). Initial pumping to high vacuum pressure was carried out in a preparation chamber immediately after thin-film preparation to avoid significant absorption of volatile impurities. The preparation chamber pressure achieved was ca. 10^{-7} mbar. The pumping times varied (1–3 h) depending upon the volume, volatile impurity content, and viscosity of the sample; i.e., viscous ionic liquids were found to require longer pumping times. The samples were then transferred to the main analytical vacuum chamber. The pressure in the main chamber remained ≤10^{-8} mbar during XPS measurements of the samples. The low chamber pressure further suggested that all volatile impurities, such as water, were removed prior to analysis.

XPS spectra were recorded using a Kratos Axis Ultra spectrometer employing a monochromated Al Kα source ($h\nu$ = 1486.6 eV), hybrid (magnetic/electrostatic) optics, a hemispherical analyzer, a multi-channel plate, and a delay line detector with an X-ray incident angle of 30° and a collection angle of 0° (both relative to the surface normal). The X-ray gun power was set to 150 W. All spectra were recorded using an aperture slot of 300 × 700 mm with a pass energy of 80 eV for survey scans and 20 eV for high-resolution core-level scans. All XPS spectra were recorded using Kratos *Vision II* software; data files were translated to VAMAS format and processed using the *CASA XPS*™

software package (version 2.3.2 and later). Binding energies (BEs) are referenced to aliphatic carbon (C 1s, 285.0 eV).

For quantitative analysis, the areas below the peak signals of the most characteristic photoemission envelopes of each element present on the surface are considered. Two point linear and Shirley background subtractions were used depending upon the overall shape of the spectrum. For C1 s and N1 s peaks, the typical shakeup contributions were not easily observed because of the low signal-to-noise ratio in the data. However, losses of 20% and 12% in the main contributions from the carbon and nitrogen peaks within the imidazolium ring can be expected as a result of the shakeup/off phenomena.[21,24] The relative sensitivity factors used were taken from the Kratos Library (RSF of F 1s = 1)[25] and were used to determine the atomic percentages. The error in these measurements, as quoted by the instrument manufacturer, is ca. 10−20% depending on the signal-to-noise ratio. Peaks were fitted using GL(30) line shapes: a combination of Gaussian (70%) and Lorentzian (30%).

The modified Auger parameter (AP) was defined as the kinetic energy of the Auger line minus the kinetic energy of the photoelectron line of a given element plus the incident photon energy. Specifically, for the Auger line applied in the definition of the AP, the most intense and sharpest feature is selected because of the ease of identification of the accurate kinetic energy, as shown in eq 1.

$$AP_{modified} = KE_{auger} − KE_{photoelectron} + h\nu$$
$$= KE_{auger} + BE_{photoelectron} \quad (1)$$

Differential Scanning Calorimetry (DSC). All scans were obtained using a TA DSC Q2000 model with a TA refrigerated cooling system 90 (RCS) and an autosampler. The samples were sealed in a glovebox in TA Tzero alodined pans with hermetic alodined lids. The temperature was ramped from 25 to 140 °C, at 5 °C min⁻¹, then stabilized at 140 °C for 5 min, subsequently cooled to −20 °C, at 5 °C min⁻¹, and then stabilized at −20 °C for 5 min, and the whole cycle was repeated three times; when polymorphism was observed, an additional four cycles were added. The DSC chamber was filled with dry dinitrogen.

Raman Spectroscopy of [C₂mim]Cl−SnCl₂. Raman spectra were recorded using a PerkinElmer RamanStation 400F spectrometer, with a 785 nm focused laser beam. In a glovebox, the neat samples were loaded into quartz cuvettes, which were subsequently sealed with parafilm. The cuvettes were removed from the glovebox immediately prior to measurement. A total of 10 scans of 5 s duration were recorded for each sample.

Crystallography of [C₂mim]Cl−SnCl₂. Crystal data for [C₂mim]-[SnCl₃] and [C₂mim]₂[SnCl₆] were collected using a Bruker Nonius Kappa CCD diffractometer with a FR591 rotating anode and a Mo target at ca. 120 K in a dinitrogen stream. Lorentz and polarization corrections were applied. The structures were solved by direct methods. Hydrogen-atom positions were located from difference Fourier maps, and a riding model with fixed thermal parameters ($U_{ij} = 1.2U_{eq}$ for the atom to which they are bonded; 1.5 for methyl) was used for subsequent refinements. The function minimized was $\sum[w(|F_o|^2 − |F_c|^2)]$ with reflection weights $w^1 = [\sigma^2|F_o|^2 + (g_1P)^2 + (g_2P)]$, where $P = [max|F_o|^2 + 2|F_c|^2]/3$. The *SHELXTL* package and *OLEX2* were used for structure solution and refinement.[26−28]

■ RESULTS AND DISCUSSION

Synthesis of the Chlorostannate(II) Ionic Liquids. Directly after preparation, chlorostannate(II) ionic liquids based on [C₈mim]⁺ were liquid for all $\chi_{SnCl_2} \leq 0.63$ compositions. A small amount of white powder (unreacted SnCl₂) was observed for $\chi_{SnCl_2} = 0.67$ and 0.75. Interestingly, when these two samples were left to cool, a significant amount of needle-shaped crystals grew in both of them within several hours. Raman spectra of the needles featured bands at 192(m), 160(s), and 126(s) cm⁻¹, which corresponds to the Raman

spectra of neat tin(II) chloride, with bands at 190(s), 160(s), and 126(s) cm⁻¹.[29] All compositions based on [C₂mim]⁺ were solid at ambient temperature. It is worth noting, for $\chi_{SnCl_2} = 0.75$, that the first needle-shaped crystals (like those found in the [C₈mim]Cl−SnCl₂ system) crystallized at ca. 60 °C; further cooling resulted in complete solidification.

In the case of both tested systems, namely, [C₈mim]Cl−SnCl₂ and [C₂mim]Cl−SnCl₂, the phase behavior was thermally reversible; i.e., heating the $\chi_{SnCl_2} = 0.67$ and 0.75 compositions resulted in complete liquefaction, and subsequent cooling again resulted in the separation of needle-shaped crystals.

Lewis Acidity and Basicity of the [C₈mim]Cl−SnCl₂ System. Parshall[6] suggested the existence of two chlorostannate(II) anions for the molten salt state: [SnCl₃]⁻ and [Sn₂Cl₅]⁻ for $\chi_{SnCl_2} > 0.50$. More recently, Illner et al.[30] studied the [C₄mim]Cl−SnCl₂ system using ¹¹⁹Sn and ¹H NMR spectroscopy, suggesting additionally the existence of [SnCl₄]²⁻ in more basic compositions. The reactions of formation of the three proposed species are shown in Table 2.

Table 2. Anions Most Likely To Be Present in Chlorostannate(II) Ionic Liquids at Particular Compositions, χ_{SnCl_2}, According to Illner et al.[30]

χ_{SnCl_2}	anions formed at different compositions
0.33	Cl⁻ + [SnCl₃]⁻ ⇌ [SnCl₄]²⁻
0.50	Cl⁻ + SnCl₂ ⇌ [SnCl₃]⁻
0.67	[SnCl₃]⁻ + SnCl₂ ⇌ [Sn₂Cl₅]⁻

It is known that chlorostannate(II) ionic liquids, like many other chlorometallate systems, may be Lewis acidic,[6] although their Lewis acidity has never been quantified. In addition, unlike for other common chlorometallates, chlorostannate(II) anions bear one or two lone pairs (see Figure 1[30]), which influence
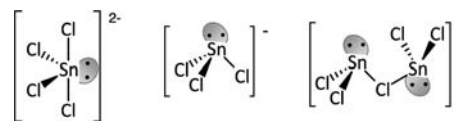
Figure 1. Schematic structures of the three chlorostannate(II) anions suggested to be present in the chlorostannate(II) ionic liquid systems.[30]

both the geometry and Lewis basicity of the ions. Illner et al.[30] investigated the changes of this basicity by monitoring the ¹H NMR chemical shift of the acidic proton in the C-2 position of the 1-butyl-3-methylimidazolium cation because it is known that in a more basic environment the proton would be less shielded (shifted downfield).[31]

The Gutmann AN is a quantitative measure of the Lewis acidity.[32] In order to measure AN, the probe molecule (tepo) was introduced into the neat liquid, and its chemical shift was measured by ³¹P NMR spectroscopy. The AN value was calculated using eq 2, where δ_{inf} is the ³¹P NMR chemical shift of the tepo signal at infinite dilution.[19]

$$AN = 2.348\delta_{inf} \quad (2)$$

In this work, the Lewis acidity of the [C₈mim]Cl−SnCl₂ system has been studied by measuring δ_{inf}, and the Lewis basicity was investigated by the ¹H NMR chemical shift of the

acidic proton in the C-2 position of the imidazolium ring of a neat ionic liquid. For the samples where white needles of tin(II) chloride precipitated, the precipitate has been removed by filtration prior to the measurements. Both chemical shifts were plotted against the composition, χ_{SnCl_2}, as shown in Figure 2.
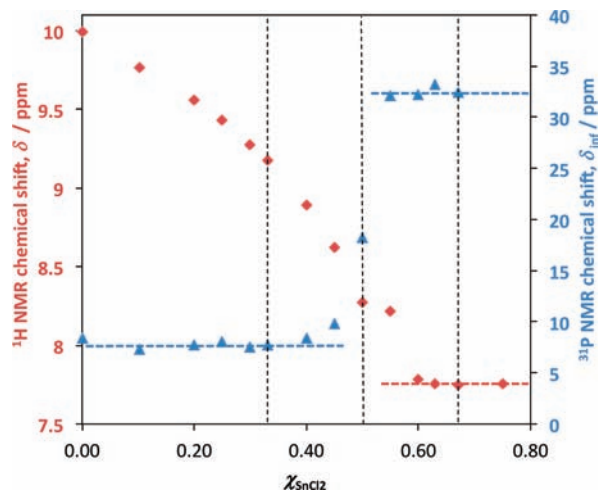
Figure 2. Plots of (▲) ^{31}P NMR shifts of tepo solutions at infinite dilution, δ_{inf}, and (◆) ^{1}H NMR chemical shifts of the acidic proton in the C-2 position of the imidazolium ring of a neat sample, as a function of χ_{SnCl_2} of the $[C_8mim]Cl-SnCl_2$ system. Dashed lines indicating plateau regions and dotted lines at χ_{SnCl_2} = 0.33, 0.50, and 0.67 are only visual guidelines. All experiments were performed at 27 °C.

For imidazolium-based ionic liquids, the chemical shift of the ^{1}H NMR signal of the proton in the C-2 position of the imidazolium ring depends strongly on the basicity of the anions, i.e., their ability to form hydrogen bonds.[31] This chemical shift for neat $[C_8mim]Cl$ is very high, ca. 10 ppm, which correlates with high Lewis basicity (strong hydrogen-bond-acceptor properties) of the chloride anion. As demonstrated in Figure 2 (red diamonds), the progressive addition of tin(II) chloride led to a gradual decrease of the chemical shift to ca. 8.3 ppm when χ_{SnCl_2} = 0.50. This behavior is related to the decreasing hydrogen-bond-acceptor ability of the anions. This

could be interpreted in terms of the formation of the less basic $[SnCl_3]^-$ and/or possibly $[SnCl_4]^{2-}$. The chemical shifts for χ_{SnCl_2} = 0.50 and 0.55 appear to be plateaued at around 8.3 ppm, and for χ_{SnCl_2} = 0.60–0.75, they approach 7.7 ppm. Most likely, the first plateau between χ_{SnCl_2} = 0.50 and 0.55 suggests a mildly Lewis basic $[SnCl_3]^-$ to be the main anion. The second one, found for χ_{SnCl_2} = 0.60–0.75, then may correspond to the formation of even less Lewis basic $[Sn_2Cl_5]^-$. Because tin(II) chloride precipitated out from both χ_{SnCl_2} > 0.63 samples, only the liquid parts of these systems could be tested; it appears that the composition of the ionic liquid for $\chi_{SnCl_2} \geq 0.63$ remained unchanged. This is comparable to our previous studies of chloroindate(III) systems, in which the composition of the liquid phase is constant for $\chi_{InCl_3} \geq 0.50$.[13c]

The plot of the chemical shift of the ^{31}P NMR signal of the Lewis acidity probe (tepo) at infinite dilution, δ_{inf}, shows two distinct ranges of acceptor properties of the $[C_8mim]Cl-SnCl_2$ system: weaker for χ_{SnCl_2} < 0.50 and stronger for χ_{SnCl_2} > 0.50, with a borderline composition (neutral) at χ_{SnCl_2} = 0.50 (see Figure 2, blue triangles). This plot strongly indicates the presence of two chlorostannate(II) anions, $[SnCl_3]^-$ and $[Sn_2Cl_5]^-$, as originally suggested by Parshall,[6] because the existence of $[SnCl_4]^{2-}$ would be visible as a major change at χ_{SnCl_2} = 0.33 in the AN versus χ_{SnCl_2} plot, as has been observed previously for chlorozincate(II) ionic liquids.[15]

From the determined δ_{inf}, AN numbers were calculated using eq 2, and the chosen values were compared to the ANs found previously for other chlorometallate systems, as shown in Figure 3.

When compared to other chlorometallate systems, chlorostannates(II) are of medium Lewis acidity, more acidic than ionic liquids based on indium(III) or than most of the chlorozincate(II) systems but less acidic than chloroaluminate-(III) and chlorogallate(III) ones. Importantly, compared to chlorozincate(II) systems,[15] chlorostannates are of much lower viscosity (vide supra), which may be crucial for reactions close to ambient temperature.

Anionic Speciation of Chlorostannate(II) Systems. Considering the contradictory data found in the literature, it
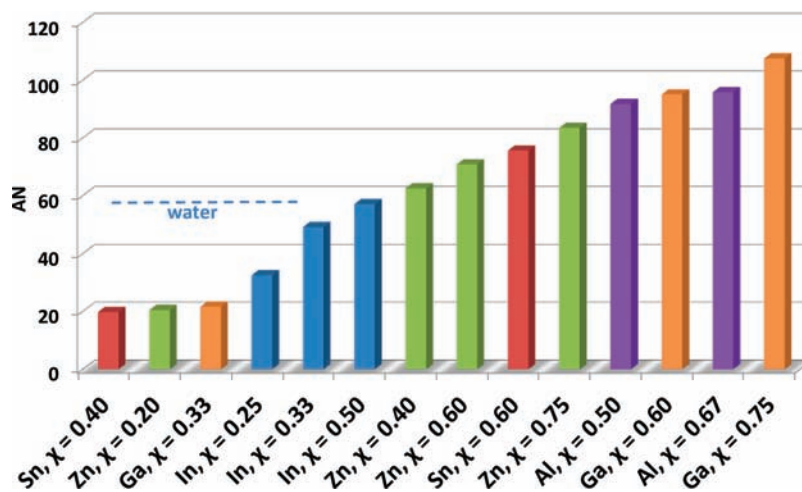
Figure 3. Comparison of ANs of selected compositions of the $[C_8mim]Cl-SnCl_2$ system (this work, red) to some compositions of other $[C_8mim]Cl-MCl_x$ systems, where M = Zn^{II}, green,[15] Ga^{III}, orange,[11] In^{III}, blue,[11] or Al^{III}, violet;[11] x = 2 for M^{II} and 3 for M^{III}.
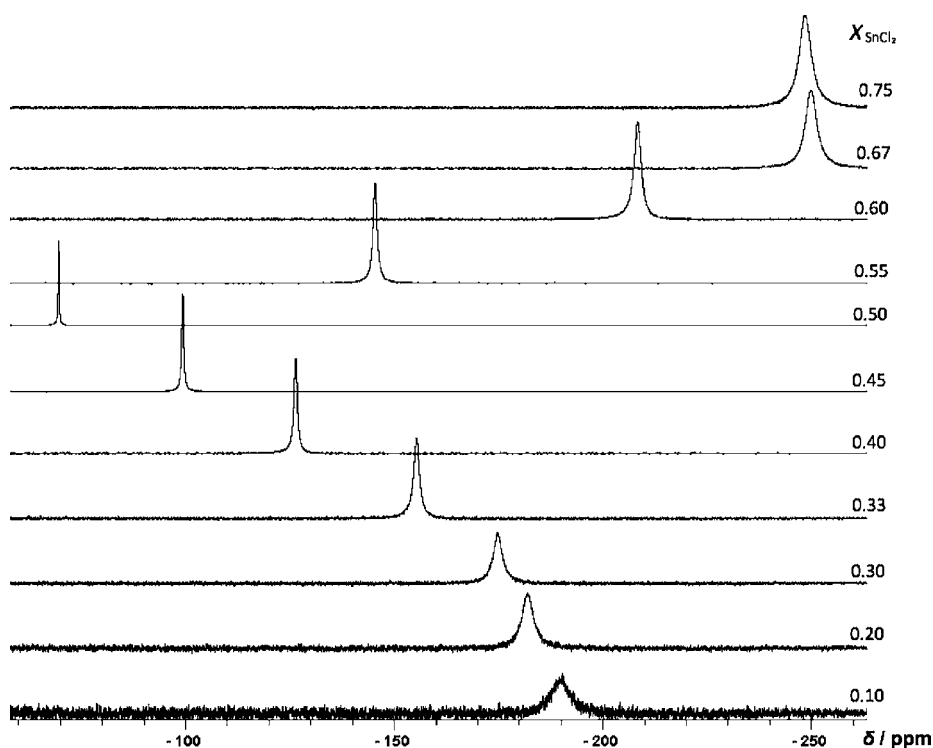
Figure 4. ^{119}Sn NMR spectra (186.48 MHz, 80 °C, neat liquid) of the $[C_8mim]Cl-SnCl_2$ system.

appeared worthwhile to conduct an in-depth study of the anionic speciation of chlorostannate(II) systems.

^{119}Sn NMR Spectroscopy of the [C$_8$mim]Cl–SnCl$_2$ System. ^{119}Sn NMR spectra of the $[C_8mim]Cl-SnCl_2$ system were recorded for a range of compositions (all samples tested as neat liquids); in all cases, only one peak has been observed, as shown in Figure 4.

Analysis of Figure 4 reveals that the width of the ^{119}Sn NMR signals varies with the composition. The peak width depends primarily on the viscosity of the medium and on the symmetry of the solution species. In order to separate the two factors, both the viscosity and peak-width at half-height (aka full width at half-maximum, fwhm) of the ^{119}Sn NMR signals, $\Delta v_{1/2}$, were plotted against the composition, as shown in Figure 5.

The sample viscosity is high in the case of very basic compositions and falls dramatically with increasing χ_{SnCl_2} to a minimum at $\chi_{SnCl_2} = 0.50$. The values of $\Delta v_{1/2}$ follow the same trend; hence, the broadening of the ^{119}Sn NMR signals toward more basic composition could be attributed to the increasing viscosity. Because an increase in the concentration of either Cl^- or $[SnCl_4]^{2-}$ may be expected to increase the viscosity compared to systems containing only $[SnCl_3]^-$, it is not possible to draw more conclusions regarding the anionic speciation in this region without additional data.

For the acidic regime, after a local maximum at $\chi_{SnCl_2} = 0.63$ is reached, the viscosity decreases to level at a rather low value of ca. 0.2 Pa s. At the same time, the increase in the peak width of the ^{119}Sn NMR signals is far more pronounced. In this case, it may be postulated that the $\Delta v_{1/2}$ values increase because of a lowering of the symmetry of the chlorostannate(II) ions from $[SnCl_3]^-$ to $[Sn_2Cl_5]^-$. A similar phenomenon has been observed for chloroaluminate(III) systems.

XPS. Because the NMR spectroscopic results were inconclusive regarding the existence of $[SnCl_4]^{2-}$ in these
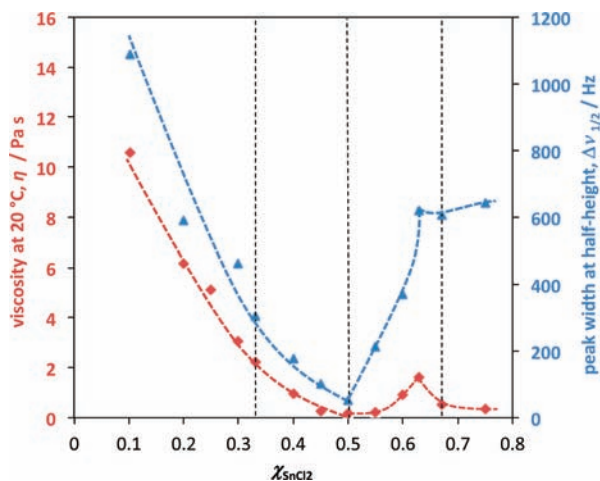
Figure 5. Plots of (▲) the viscosity of the $[C_8mim]Cl-SnCl_2$ system at 20 °C, η, and (◆) peak width at half-height of ^{119}Sn NMR signals, $\Delta v_{1/2}$, measured for the $[C_8mim]Cl-SnCl_2$ system at 80 °C, plotted as functions of the composition, χ_{SnCl_2}. Dashed trend lines and dotted lines at $\chi_{SnCl_2} = 0.33$, 0.50, and 0.67 are only visual guidelines.

systems, an additional spectroscopic probe was invoked. XPS was used to study three compositions of the $[C_8mim]Cl-SnCl_2$ system, $\chi_{SnCl_2} = 0.33$, 0.50, and 0.67 (see Table 2).

The sample composition and purity were established by measurement of the XPS survey and high-resolution spectra for each sample studied. The survey scans confirmed that the measured stoichiometry was within acceptable levels of experimental error from that calculated for each sample. XPS signals were observed for each of the expected elements, and there was no evidence for the presence of surface-segregated contaminants including silicones, hydrocarbons, or oxygenates. Accurately determined BE data for each element, in each

Table 3. BEs ($\pm$0.1 eV) of Different Atoms for Chlorostannate(II) Containing Ionic Liquids

χ_{SnCl_2}	Sn $3d_{5/2}$	N 1s	C^2 1s	C^{4,5} 1s	C^{6,7} 1s	C$_{aliphatic}$ 1s (C$^{8-14}$)	Cl $2p_{3/2}$^{a}	Cl $2p_{3/2}$^{b}
0.67	487.3	401.9	287.5	286.8	286.3	285.0	198.7	
0.50	487.1	401.9	287.5	286.8	286.4	285.0	198.6	
0.33	487.0	401.8	287.4	286.7	286.2	285.0	198.5	197.2
0.00		401.7	287.3	286.7	286.1	285.0		197.1

^{a}Cl component corresponding to chlorostannate(II) anions. ^{b}Cl component corresponding to Cl$^-$. Note: all BEs are measured after charge correction of the raw data by setting the BE of C$_{aliphatic}$ 1s to 285.0 eV.

sample, are presented in Table 3. These data were extracted from higher-resolution, element-specific scans, where all BEs are charge-corrected by setting the observed BE of the easily identifiable C$_{aliphatic}$ 1s component to 285.0 eV (this includes contributions for C8−14; see Figure 6).
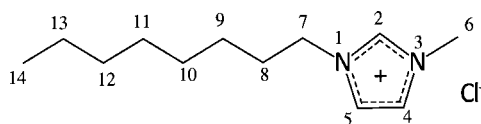
Figure 6. Structure presenting the numbering system used in the deconstruction and fitting of the C 1s photoemission envelope of imidazolium-based ionic liquids.

The absolute error in the acquisition of BEs is $\pm$0.1 eV; consequently, any variation in the corrected BE $\geq$ 0.2 eV may be considered as real. BE data for pure [C$_8$mim]Cl (i.e., when χ_{SnCl_2} = 0.00) is also included in the table for ease of reference.

The high-resolution Cl 2p XPS spectra of the three materials studied, i.e., χ_{SnCl_2} = 0.33, 0.50, and 0.67, are illustrated in Figure 7. The spectra have been normalized to the area of the N 1s peak for the sample when χ_{SnCl_2} = 0.50. For reference purposes, the Cl 2p XPS spectrum for pure [C$_8$mim]Cl, i.e., χ_{SnCl_2} = 0.00, is also included.

The Cl 2p XPS spectrum of the χ_{SnCl_2} = 0.67 sample (Figure 7a) reveals a single electronic environment for chlorine with a BE of 198.6 eV; this photoemission is to the [SnCl$_3$]$^-$ anion. Similarly, the XPS spectrum of the sample when χ_{SnCl_2} = 0.50 (Figure 7b) shows only a single chlorine component with a BE that is within experimental error of that observed in Figure 7a. By comparison, the Cl 2p XP spectrum of the sample when χ_{SnCl_2} = 0.33 (Figure 7c) reveals two discrete electronic environments, suggesting that the material is, in fact, a mixture. The ratio of the area of the lower BE contribution (Cl $2p_{3/2}$ BE = 197.2 eV) to that at higher BE (Cl $2p_{3/2}$ BE = 198.5 eV) is 1:3, respectively. The photoemission peaks for both contributions are observed as spin−orbit-coupled doublets with a consistent energy separation of 1.6 eV. The XPS spectrum of the lower BE component (Cl $2p_{3/2}$ BE = 197.2 eV) was similar, certainly within acceptable experimental error, to that of [C$_8$mim]Cl. The Cl 2p XPS spectrum of pure [C$_8$mim]Cl is included as Figure 7d for comparison. The XPS spectrum corresponding to the higher BE contribution (Cl $2p_{3/2}$ BE = 198.5 eV) was identical with that exhibited for the samples when χ_{SnCl_2} = 0.50 and 0.67, i.e., Figures 7a and 6b.

The measured Cl $2p_{3/2}$ BEs, when considered with the area ratios for the two components, suggest that the sample where χ_{SnCl_2} = 0.33 is an equimolar mixture of Cl$^-$ (lower BE) and [SnCl$_3$]$^-$ (higher BE) anions; i.e., there is no experimental
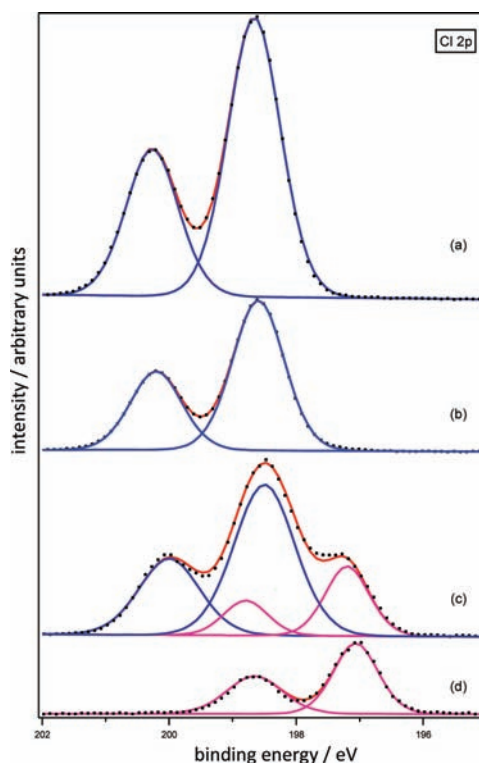
Figure 7. XPS spectra with fitting of Cl 2p for various compositions of the [C$_8$mim]Cl−SnCl$_2$ system for χ_{SnCl_2} = (a) 0.67, (b) 0.50, and (c) 0.33 and for (d) the neat [C$_8$mim]Cl. The intensities are normalized to the intensity of the N$_{cation}$ 1s fitted peak for the χ_{SnCl_2} = 0.50 composition. All XPS spectra were charge-corrected by referencing the aliphatic C 1s photoemission peak (C$_{aliphatic}$ 1s) to 285.0 eV.

evidence to suggest the presence of [SnCl$_4$]$^{2-}$ in this sample. Full BE data for all samples investigated here are also presented in Table 3 to aid the direct comparison. On the basis of these data, it has not been possible to confirm the presence or absence of [Sn$_2$Cl$_5$]$^-$ in the sample when χ_{SnCl_2} = 0.67.

The high-resolution Sn $3d_{5/2}$ XPS spectra of the same three samples are shown in Figure 8.

The spectrum of the sample when χ_{SnCl_2} = 0.33 (blue curve, Figure 8) reveals a single electronic environment for tin, with a BE of 487.0 eV. The spectrum obtained for the χ_{SnCl_2} = 0.50 sample (black curve, Figure 8) was again very similar to that of χ_{SnCl_2} = 0.33, with the Sn $3d_{5/2}$ BEs of both compositions within experimental error (see Table 3). This supported the observations made in the Cl 2p XPS spectra, strongly suggesting the presence of a single chlorostannate(II) anion, [SnCl$_3$]$^-$, in both samples. The XPS spectrum of the sample when χ_{SnCl_2} = 0.67 (red curve, Figure 8) is visibly shifted toward a higher BE. However, the change in the BE is relatively small
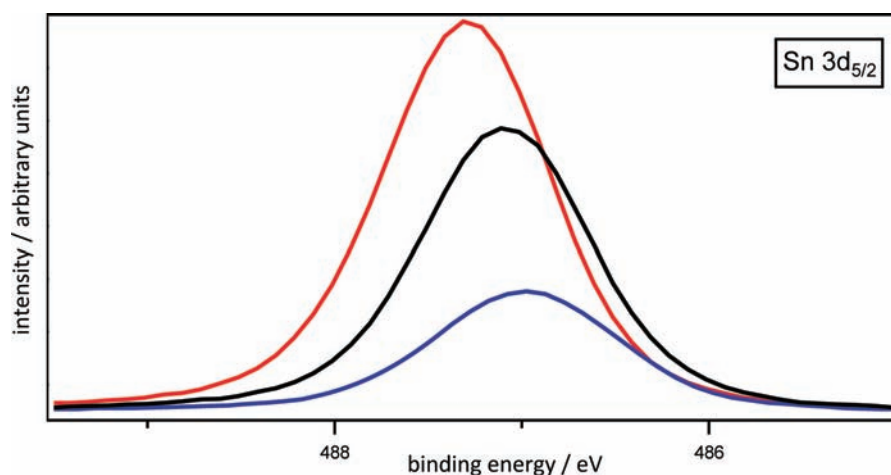
Figure 8. XPS spectra of Sn $3d_{5/2}$ for the three compositions χ_{SnCl_2} = 0.33 (blue), 0.50 (black), and 0.67 (red). The intensities are normalized to the intensity of the N_{cation} 1s fitted peak for the χ_{SnCl_2} = 0.50 composition. All XPS spectra were charge-corrected by referencing the aliphatic C 1s photoemission peak ($C_{aliphatic}$ 1s) to 285.0 eV. Sn $3d_{3/2}$ has been omitted from these data; a consistent energy separation of 8.4 eV was noted between the two components of this spin−orbit-coupled doublet.

and cannot be quantified absolutely because it is within the experimental error of the spectrum measured when χ_{SnCl_2} = 0.50. Consequently, it is not possible to make any further conclusions based upon these data alone because the BEs are statistically very similar.

Because the experimental error associated with measurement of the BEs is on the order of ±0.1 eV, it is difficult to distinguish, with any degree of confidence, different electronic environments with BE shifts of only 0.2 eV.[22] An alternative method, which may be employed in cases where only small BE shifts are observed, is a comparison of the AP for each sample. Changes in the AP can be as much as 3 times larger than the associated photoemission shift and, more significantly, the level of error in the measurement is much smaller, ±0.05 eV. Furthermore, the AP is not influenced by sample charging, which has been noted in other ionic liquid systems.[23] Table 4

Table 4. APs (eV) for Tin in Three Compositions of the $[C_8mim]Cl$−$SnCl_2$ System, Namely, χ_{SnCl_2} = 0.33, 0.50, and 0.67

χ_{SnCl_2}	Sn $3d_{5/2}$ BE	Sn MNN KE[a]	AP
0.33	487.0	431.7	918.7
0.50	487.1	431.6	918.7
0.67	487.3	431.7	919.0

[a]Sn MNN is the most prominent Auger transition noted in the measured samples; it is used in conjunction with the most prominent photoemission, in this case Sn $3d_{5/2}$, to calculate the AP.

lists the AP values measured for the three compositions of the $[C_8mim]Cl$−$SnCl_2$ system. These data confirm that the electronic environments of tin are identical when χ_{SnCl_2} = 0.33 and 0.50, further supporting that both compositions contain $[SnCl_3]^-$ as the only chlorostannate(II) anion. The AP for the tin in the χ_{SnCl_2} = 0.67 sample is at a higher energy, which suggests a more electron-deficient environment, supporting the presence of $[Sn_2Cl_5]^-$.

DSC of the $[C_2mim]Cl$−$SnCl_2$ System. The long alkyl chain on the cation of the $[C_8mim]Cl$−$SnCl_2$ system frustrates crystallization, yielding room temperature ionic liquids. This

makes it more difficult to obtain a well-defined phase diagram because glass transitions instead of melting points were observed.

The DSC scans proved to be fairly complex, most featuring several peaks. On the basic side, lower melting points were observed on the first scan, and then a higher melting point was consistently found at each composition in the subsequent scans. This could be typically ascribed either to polymorphism[33] or to a change in speciation, forming $[SnCl_4]^{2-}$ anions. To investigate this further, a χ_{SnCl_2} = 0.20 sample was removed from the DSC pan immediately after six heating−cooling cycles (Figure 9a) and the Raman spectrum was measured and compared with that of the initial sample (Figure 9b).

Aside from the quality loss due to the very small amount of the sample, no difference in the Raman signals was observed, supporting the assignment of phases I and II, as well as phases IV and V (Figure 10), as polymorphs.

The phase diagram (Figure 10) features a peritectic point at χ_{SnCl_2} = 0.50, corresponding to pure $[C_2mim][SnCl_3]$, and a eutectic point at χ_{SnCl_2} = 0.33 (equimolar mixture of $[SnCl_3]^-$ and Cl^-). In the acidic region, a eutectic point is found at ca. χ_{SnCl_2} = 0.64, with $[SnCl_3]^-$ and $[Sn_2Cl_5]^-$ as the primary anionic components.

Raman Spectroscopy of the $[C_2mim]Cl$−$SnCl_2$ System. It has been conclusively demonstrated by spectroscopic means that chlorostannate(II) ionic liquids contain three anions in equilibrium with each other: Cl^-, $[SnCl_3]^-$, and $[Sn_2Cl_5]^-$. At the same time, the literature data regarding speciation of such ionic liquids in the crystalline phase were not conclusive.

Literature Data. Raman spectroscopy of three compositions (χ_{SnCl_2} = 0.33, 0.50, and 0.67) of the $[C_2mim]Cl$−$SnCl_2$ system (solid), coupled with density functional theory calculations, revealed the existence of $[SnCl_3]^-$ anions in the first two samples and of both $[SnCl_3]^-$ and $[Sn_2Cl_5]^-$ in the last one.[34] No $[SnCl_4]^{2-}$ has been detected. Interestingly, on the basis of the crystal structure database (CCSD) search, a crystal structure of a chlorostannate(II) salt containing only $[Sn_2Cl_5]^-$ as a unique chlorostannate(II) anion has never been observed; the only structure featuring a discrete $[Sn_2Cl_5]^-$
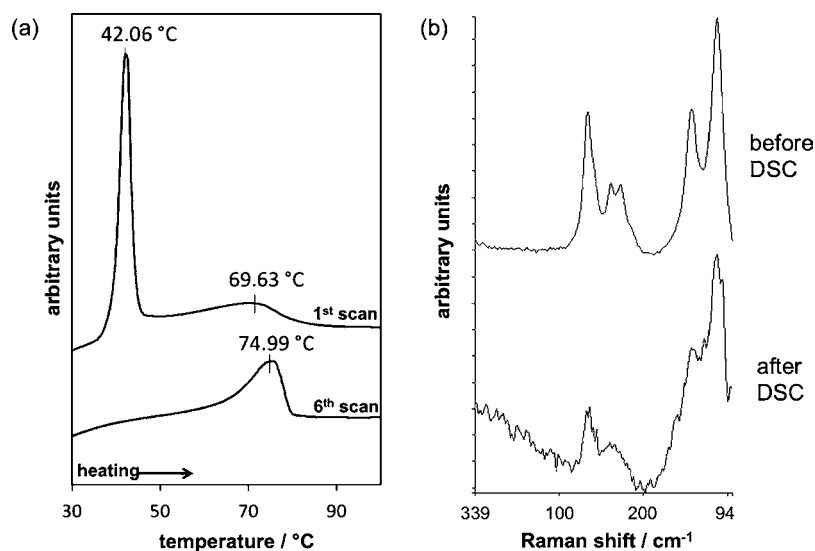
Figure 9. Analysis of the $\chi_{SnCl_2} = 0.20$ composition: (a) fragments of DSC traces for the first and sixth scans; (b) Raman spectra before and immediately after the DSC experiment was carried out.
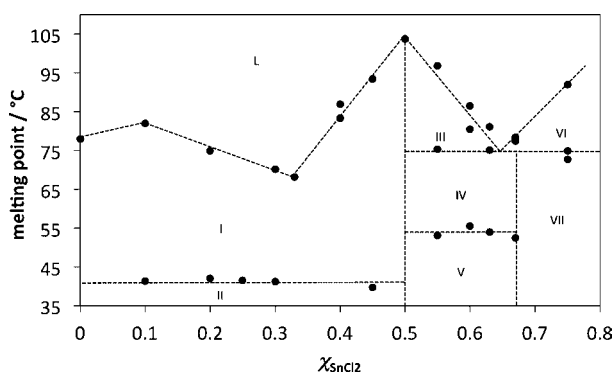
Figure 10. Phase diagram of the $[C_2mim]Cl-SnCl_2$ system: (I and II) $[C_2mim][SnCl_3]$ + $[C_2mim]Cl$; (III) $[C_2mim][SnCl_3]$ + L; (IV and V) $[C_2mim][SnCl_3]$ + $[C_2mim][Sn_2Cl_5]$; (VI) $SnCl_2$ + L; (VII) $[C_2mim][Sn_2Cl_5]$ + $SnCl_2$. The dotted lines are only visual guidelines.

anion also contains $[SnCl_3]^-$ (Figure 11b).[35] However, a crystal structure of $[C_4mim]_2[SnCl_4]$, with an anion of distorted C_{2v}
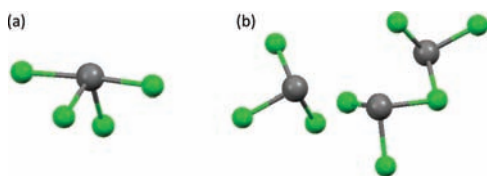
Figure 11. Crystal structures of chlorostannate(II) anions: (a) $[SnCl_4]^{2-}$;[36] (b) $[SnCl_3]^-$ cocrystallized with $[Sn_2Cl_5]^-$.[35]

symmetry, has been obtained from the $[C_4mim]Cl-SnCl_2$ system of $\chi_{SnCl_2} = 0.33$ composition, when crystals were grown from a diethyl ether solution at 245 K (Figure 11a).[36] Furthermore, crystals of a range of alkylammonium chlorostannate(II) salts, $\chi_{SnCl_2} = 0.33$, also grown from solution, were tested using Raman spectroscopy, X-ray absorption fine structure, and X-ray diffractometry (both powder and single crystal), with the $[SnCl_4]^{2-}$ anion being the only detected chlorostannate(II) species, both spectroscopically and crystallographically.[37]

This Work. The Raman spectra of a range of compositions of the $[C_2mim]Cl-SnCl_2$ system were acquired at ambient temperature, the vibrational frequencies in the region characteristic of $\nu(Sn-Cl)$ stretching shown in Figure 12, and listed in Table 5. These results were in agreement with the literature data for the same system.[34]

For $\chi_{SnCl_2} < 0.50$, the only detected chlorostannate(II) anion was $[SnCl_3]^-$, with the $\nu_1(Sn-Cl)$ vibration at 265 ± 1 cm^{-1} (see Table 5), which is in agreement with literature data, in which $\nu_1(Sn-Cl) = 263$ cm^{-1}.[29] Despite testing several samples with a high chloride ion concentration, no $[SnCl_4]^{2-}$ was found
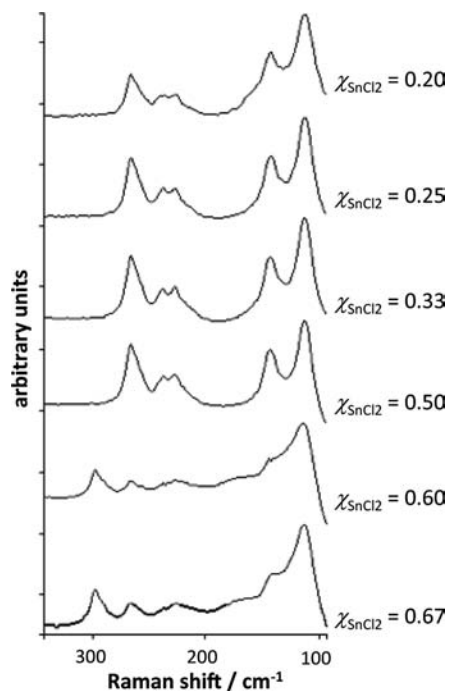
Figure 12. Raman spectra of the $[C_2mim]Cl-SnCl_2$ system (ambient temperature, solid state), where the χ_{SnCl_2} values are quoted in the figure.

Table 5. Raman Frequencies $(\text{cm}^{-1})^a$ of the Chlorostannate(II)-Related Peaks Obtained for χ_{SnCl_2} = 0.20−0.67 Composition of $[C_2mim]Cl−SnCl_2$

	χ_{SnCl_2}					
assignment	0.2	0.25	0.33	0.5	0.6	0.67
$[SnCl_3]^-$	266(s)	266(s)	265(s)	266(s)	265(s)	265(s)
		258(sh)	257(sh)	259(sh)	256(m)	259(sh)
	237(m)	238(m)	238(m)	238(m)	237(w)	238(w)
	227(m)	226(m)	227(m)	227(m)	226(m)	226(m)
	142(s)	143(s)	142(s)	143(s)	144(m)	141(m)
	112(s)	112(s)	112(s)	112(s)	113(s)	113(s)
$[Sn_2Cl_5]^-$					298(s)	298(s)
					291(sh)	292(sh)
					217(w)	217(w)
					210(w)	212(w)

^{a}The intensities of the peaks are represented in parentheses (s = strong, m = medium, w = weak, and sh = shoulder).

in the solid state [i.e., no $\nu_1(Sn−Cl)$ = 332 cm^{-1} has been observed].[37] It is most likely that whereas trichlorostannate(II) is the main species present in the liquid phase, and as such crystallizes from the melt, crystallization from a molecular solvent promotes formation of the tetrachlorostannate(II) anion.

As a matter of fact, according to the Kapustinskii equation,[38] a $[SnCl_4]^{2-}$-based salt will have a higher lattice energy because of the doubly charged anion and therefore crystallizes more readily. This is facilitated when a polar solvent, such as ethanenitrile, partially screens the effect of the free ion pair on the tin atom and solvates the doubly charged $[SnCl_4]^{2-}$ (Figure 1).

As was already discussed, an excess of tin(II) chloride crystallized out from χ_{SnCl_2} = 0.67 composition in the shape of long needles before the bulk of the sample solidified. To obtain a Raman spectrum of the bulk, the needles were allowed to settle on the bottom of the vial in an elevated temperature, and then the temperature was decreased, so that the bulk sample could solidify. A sample for the Raman spectroscopy test was then collected from the top of the solidified chlorostannate(II) ionic liquid.

As shown in Figure 12, both χ_{SnCl_2} > 0.50 spectra are very similar and feature two sets of peaks, corresponding to $[SnCl_3]^-$ and $[Sn_2Cl_5]^-$, as was observed and assigned for the χ_{SnCl_2} = 0.67 composition of the same system by Matsuzawa et al.[34] As listed in Table 5, the $\nu_1(Sn−Cl)$ vibration of $[SnCl_3]^-$ (265 ± 1 cm^{-1}) is still present, while a new set of vibrations, including the $\nu_1(Sn−Cl)$ vibration of $[Sn_2Cl_5]^-$ (298 cm^{-1}), has appeared. It appears that, although tin(II) chloride may dissolve in hot chlorostannate(II) ionic liquids up to χ_{SnCl_2} = 0.67, there is a strong preference for this system to remain a mixture of both chlorostannate(II) anions, in the liquid and solid states. This finds confirmation in the observed crystallization of $SnCl_2$ needles from χ_{SnCl_2} > 0.60 compositions and in the crystals found in the organic CCSD, where the only crystal structures containing a $[Sn_2Cl_5]^-$ unit contain also a $[SnCl_3]^-$ unit, in a 1:1 molar ratio, i.e. analogous to χ_{SnCl_2} = 0.60, which seems to be strongly thermodynamically favored.[35]

Crystallography. A sample of the $[C_2mim]Cl−SnCl_2$ system, χ_{SnCl_2} = 0.67, has been analyzed using single-crystal X-ray diffractometry. Interestingly, the first crystal to be measured revealed the existence of pure $[C_2mim][SnCl_3]$,

which corresponds to a χ_{SnCl_2} = 0.50 composition. The surrounding and hydrogen-bonding interactions of the crystallographically equivalent $[C_2mim]^+$ cations and the $[SnCl_3]^-$ anions are shown in Figure 13, while the crystallographic data are summarized in Table 6.

The $[SnCl_3]^-$ anions are surrounded by three imidazolium cations that form C−H···Cl hydrogen-bonding interactions, with distances ranging from 2.770 to 3.031 Å. Because tin(II) in
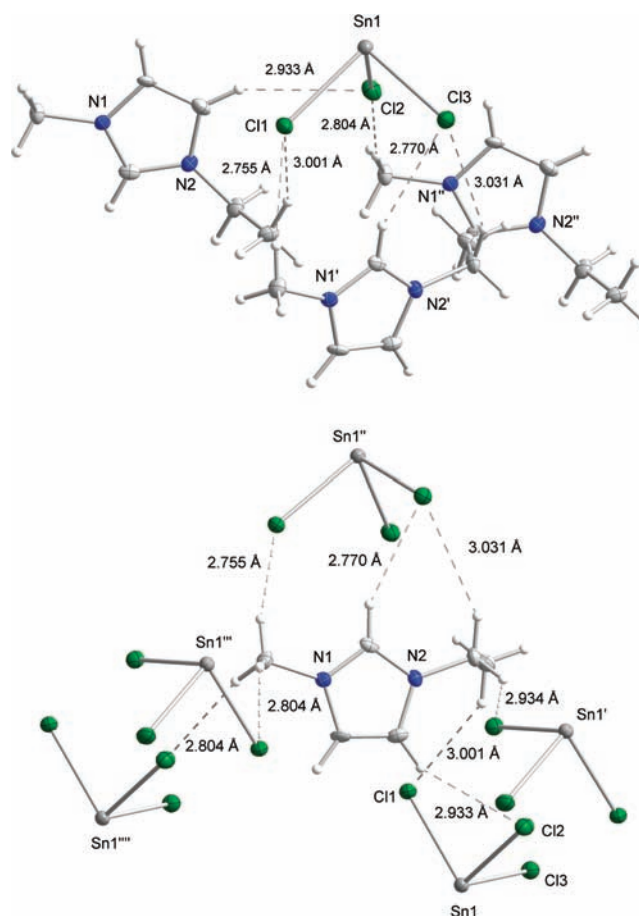
Figure 13. Crystal structure of $[C_2mim][SnCl_3]$, showing the hydrogen-bonding interactions of the 1-ethyl-3-methylimidazolium cation and the $[SnCl_3]^-$ anion (top) and the surrounding interactions of the anions around the cation (bottom).

Table 6. Crystallographic Data for $[C_2mim][SnCl_3]$ and $[C_2mim]_2[SnCl_6]$

	$[C_2mim][SnCl_3]$	$[C_2mim]_2[SnCl_6]$
formula	$C_6H_{11}Cl_3N_2Sn$	$C_{12}H_{22}Cl_6N_4Sn$
MW/g	336.21	553.73
dimens/mm	$0.10 \times 0.06 \times 0.05$	$0.01 \times 0.12 \times 0.24$
cryst syst	orthorhombic	orthorhombic
space group	$P2_12_12_1$	$Pcba$
a/Å	8.333(3)	9.430(3)
b/Å	9.134(4)	14.241(5)
c/Å	14.611(7)	15.465(5)
α/deg	90.00	90.00
β/deg	90.00	90.00
γ/deg	90.00	90.00
V/Å^3	1112.1(8)	2077.0(11)
Z	4	4
D_{calc}/g cm^{-3}	2.008	1.771
cryst shape	block	plate
cryst color	colorless	colorless
μ/mm^{-1}	2.971	2.004
$F(000)$	648.0	1096
no. of measd reflns	6619	15301
no of unique reflns	2537	2384
no. of param refined	111	108
GOF on F^2	0.996	0.939
R1	0.0274	0.0319
wR2	0.0424	0.1212
CCDC	xxxxx	xxxxx

the $[SnCl_3]^-$ anion possesses a lone pair of electrons, it has a trigonal-pyramidal structure with three inequivalent chlorine atom sites, with the Sn−Cl distances ranging from 2.507(1) to 2.572(1) Å. This is within a typical range for trichlorostannate-(II) anions, which is 2.502 ± 0.056 Å (calculated from 35 structures in the CSD).[39]

Oxidative Stability. It has long been known that chlorostannate(II) ionic liquids, both in the liquid and solid states, are prone to oxidation with atmospheric oxygen,[6] which particularly applies to the Lewis basic samples, having an excess of chloride ions. For example, the Raman spectrum of the χ_{SnCl_2} = 0.20 composition of the $[C_2mim]Cl–SnCl_2$ system, exposed overnight to the atmosphere, revealed a strong band at 310 cm^{-1}, corresponding to the ν_1(Sn−Cl) vibration in $[SnCl_6]^{2-}$.[29] At the same time, a strong band at 298 cm^{-1}, found in the unoxidized sample and assigned to the ν_1(Sn−Cl) vibrations in $[SnCl_3]^-$,[29] disappeared from the spectrum. A single-crystal structure of the oxidation product, $[C_2mim]_2[SnCl_6]$, was

obtained and is shown in Figures 14 and 15; crystallographic data are presented in Table 6.

The crystal structure of $[C_2mim]_2[SnCl_6]$ consists of discrete $[C_2mim]^+$ cations and $[SnCl_6]^{2-}$ anions. The $[SnCl_6]^{2-}$ anions are surrounded by eight imidazolium cations that form C−H···Cl hydrogen-bonding interactions, with distances ranging from 2.801 to 2.882 Å. Of interest is the fact that only the α-hydrogen atoms on the alkyl groups and the H-4 and H-5 protons of the ring partake in hydrogen bonding; there is no interaction with the most acidic H-2 proton on the ring. The slightly distorted octahedral $[SnCl_6]^{2-}$ anions have three inequivalent chlorine atom sites, with Sn−Cl distances ranging from 2.430(1) to 2.437(1) Å and Cl−Sn−Cl angles ranging from 89.61(3)° to 90.38(3)°. The geometry is typical for $[SnCl_6]^{2-}$ anions found in the literature, with bond lengths within the range of 2.429 ± 0.021 Å (calculated from 112 structures in the CSD).[39]

■ CONCLUSIONS

The Lewis acidity of chlorostannate(II) systems, expressed as AN, was measured for a range of compositions. It has been demonstrated that $\chi_{SnCl_2} < 0.50$ samples have very weak acceptor properties, whereas the $\chi_{SnCl_2} > 0.50$ compositions are Lewis acids and their acidities are similar to that of chlorozincate(II) systems and weaker than that of chlorogallate(III) or chloroaluminate(III) ones. The $\chi_{SnCl_2} = 0.50$ composition may be considered as neutral. The Lewis basicity decreased with a decrease in the amount of free chloride in basic samples, to reach a plateau for acidic compositions.

The only anions detected in neat chlorostannate(II) systems, both in the solid and liquid phases, were Cl$^-$ and $[SnCl_3]^-$ in the basic regime and $[SnCl_3]^-$ and $[Sn_2Cl_5]^-$ in the acidic regime. Trichlorostannate(II) anion is the sole anionic component of the $\chi_{SnCl_2} = 0.50$ composition. No $[SnCl_4]^{2-}$ anions were found in either the liquid or solid state, although such an anion has been reported in the literature for systems crystallized from an organic solvent (ethanenitrile).[37]

There are several features characteristic of chlorostannate(II) systems compared to more classical chlorometalate ionic liquids. First, although hot chlorostannates(II) dissolve tin(II) chloride to form a homogeneous liquid up to $\chi_{SnCl_2} = 0.67$, excess of tin(II) chloride recrystallizes in the form of long needles from all $\chi_{SnCl_2} > 0.63$ compositions. Consequently, acidic samples of chlorostannate(II) ionic liquids tend to contain both $[SnCl_3]^-$ and $[Sn_2Cl_5]^-$ instead of the pure dimer.
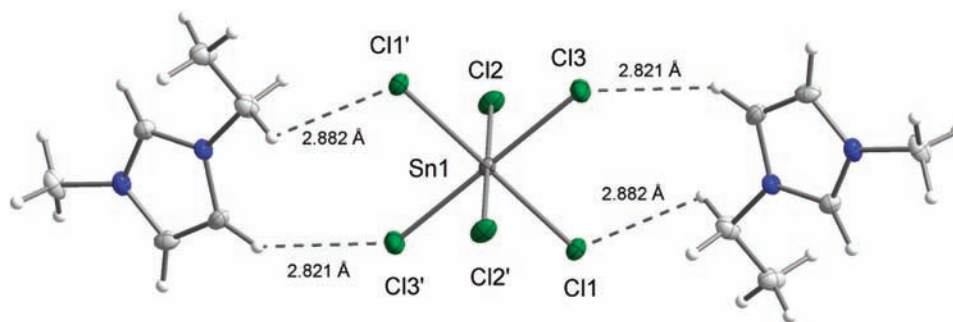
Figure 14. Partial crystal structure of $[C_2mim]_2[SnCl_6]$ showing hydrogen-bonding interactions between two 1-ethyl-3-methylimidazolium cations and the $[SnCl_6]^{2-}$ anion.
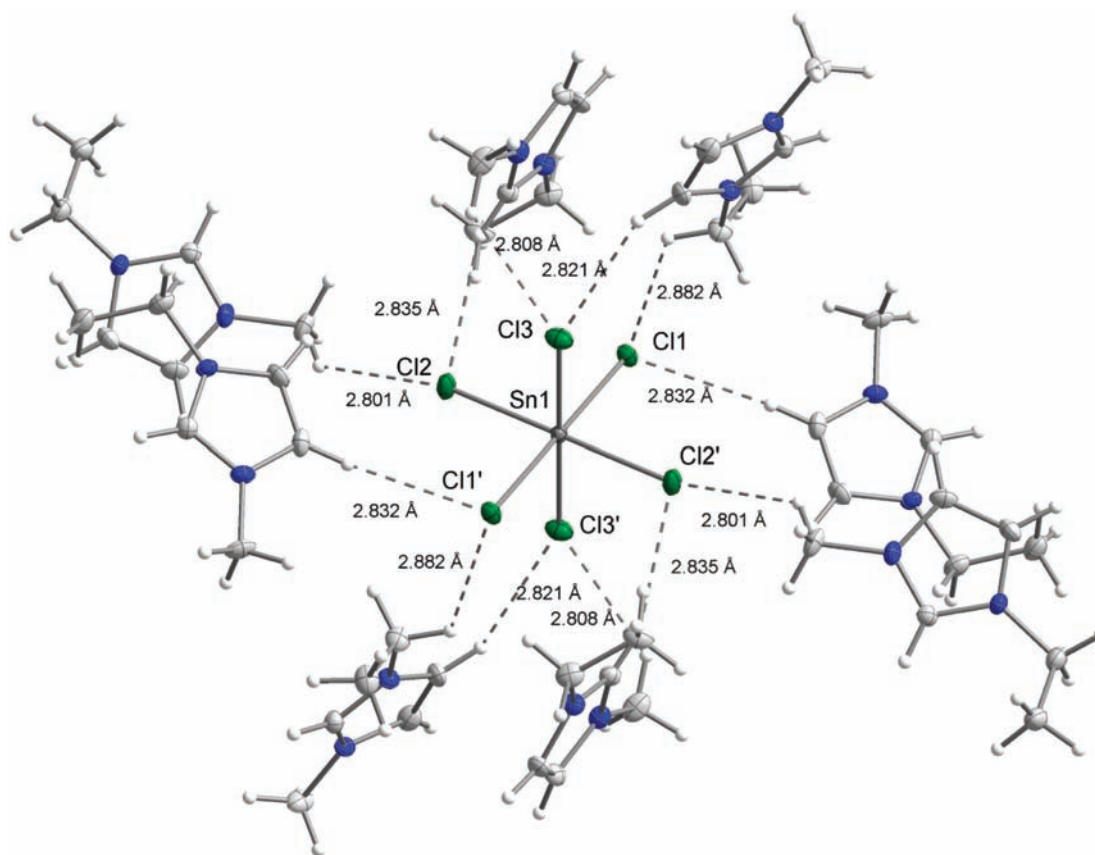
Figure 15. Crystal structure of [C₂mim]₂[SnCl₆] showing all hydrogen-bonding interactions between the 1-ethyl-3-methylimidazolium cations and the [SnCl₆]²⁻ anion.

Second, for basic samples, the anionic speciation of the crystalline systems depends on the method of crystallization; i.e., crystallized from the melt, the χ_{SnCl_2} = 0.33 composition will contain in bulk equimolar amounts of Cl⁻ and [SnCl₃]⁻ anions, whereas the same composition crystallized from a molecular solvent is likely to be comprised solely of [SnCl₄]²⁻ anions (and their counterions). Finally, not only are chlorostannates(II) prone to oxidation in air, but provided enough free chlorides are around, they oxidize to produce another family of ionic liquids, chlorostannates(IV), based on [SnCl₆]²⁻ anions.

ASSOCIATED CONTENT

Ⓢ Supporting Information

X-ray crystallographic data in CIF format. This material is available free of charge via the Internet at http://pubs.acs.org.

AUTHOR INFORMATION

Corresponding Author

*E-mail: peter.licence@nottingham.ac.uk (P.L.), quill@qub.ac.uk (M.S.-K.).

Present Address

‡CERTECH asbl, Rue Jules Bordet, Zone Industrielle C, B-7180 Seneffe, Belgium.

Notes

The authors declare no competing financial interest.

REFERENCES

(1) Plechkova, N. V.; Seddon, K. R. *Chem. Soc. Rev.* **2007**, *37*, 123.
(2) Hallett, J. P.; Welton, T. *Chem. Rev.* **2011**, *111*, 3508.
(3) Bica, K.; Gaertner, P. *Org. Lett.* **2006**, *8*, 733.
(4) Atkins, M. P.; Seddon, K. R.; Swadźba-Kwaśny, M. *Pure Appl. Chem.* **2011**, *83*, 1391.
(5) Gunaratne, H. Q. N.; Lotz, T. J.; Seddon, K. R. *New J. Chem.* **2010**, *34*, 1821.
(6) Parshall, G. W. *J. Am. Chem. Soc.* **1972**, *94*, 8716.
(7) Wasserscheid, P.; Waffenschmidt, H. *J. Mol. Catal. A: Chem.* **2000**, *164*, 61.
(8) Wang, H.; Lu, B.; Wang, X.; Zhang, J.; Cai, Q. *Fuel Process. Technol.* **2009**, *90*, 1198.
(9) Kadokawa, J.; Iwasaki, I.; Tagaya, H. *Macromol. Rapid Commun.* **2002**, *23*, 757.
(10) Kohler, F.; Roth, D.; Kuhlmann, E.; Wasserscheid, P.; Haumann, M. *Green Chem.* **2010**, *12*, 979.
(11) Estager, J.; Oliferenko, A. A.; Seddon, K. R.; Swadźba-Kwaśny, M. *Dalton Trans.* **2010**, *39*, 11375.
(12) (a) Hussey, C. L. *Adv. Molten Salt Chem.* **1983**, *5*, 185. (b) Tsuda, T.; Hussey, C. L. In *Modern Aspects of Electrochemistry*; White, R. I., Vayenas, C. G., Gamboa-Aldeco, M. E., Eds.; Springer:

1720

dx.doi.org/10.1021/ic300241p | *Inorg. Chem.* 2013, 52, 1710−1721

Dordrecht, The Netherlands, 2009; Vol. *45*, p 63. (c) Øye, H. A.; Jagatoyen, M.; Oksefjel, T.; Wilkes, J. S. *Mater. Sci. Forum* **1991**, *73–75*, 183.

(13) (a) Carpenter, M. K.; Verbrugge, M. W. *J. Mater. Res.* **1994**, *9* (10), 2584. (b) Yang, J. Z.; Tian, P.; Xu, W. G.; Xu, B.; Liu, S. Z. *Thermochim. Acta* **2004**, *412* (1–2), 1. (c) Apperley, D. C.; Hardacre, C.; Licence, P.; Murphy, R. W.; Plechkova, N. V.; Seddon, K. R.; Srinivasan, G.; Swadźba-Kwaśny, M.; Villar-Garcia, I. J. *Dalton Trans.* **2010**, *39*, 8679.

(14) (a) Wicelinski, S. P.; Gale, R. J.; Wilkes, J. S. *Thermochim. Acta* **1988**, *126*, 255. (b) Wicelinski, S. P.; Gale, R. J.; Williams, S. D.; Mamantov, G. *Spectrochim. Acta, Part A* **1989**, *45*, 759. (c) Wicelinski, S. P.; Gale, R. J.; Pamidimukkala, K. M.; Lane, R. A. *Anal. Chem.* **1988**, *60*, 2228. (d) Hardacre, C.; Murphy, R. W.; Seddon, K. R.; Srinivasan, G.; Swadźba-Kwaśny, M. *Aust. J. Chem.* **2010**, *63*, 845.

(15) Estager, J.; Nockemann, P.; Seddon, K. R.; Swadźba-Kwaśny, M.; Tyrrell, S. *Inorg. Chem.* **2011**, *50*, 5258.

(16) (a) Zawodzinski, T. A., Jr.; Osteryoung, R. A. *Inorg. Chem.* **1989**, *28*, 1710. (b) Mantz, R. A.; Trulove, P. C.; Carlin, R. T.; Theim, T. L.; Osteryoung, R. A. *Inorg. Chem.* **1997**, *36*, 1227.

(17) Wilkes, J. S.; Levisky, J. A.; Hussey, C. L.; Druelinger, M. L. *Proc. Int. Symp. Molten Salts* **1980**, *81–89*, 245.

(18) *Handbuch der Präparativen Anorganischen Chemie*, 3rd ed.; Brauer, G.; Ed.; Ferdinand Enke Verlag: Stuttgart, Germany, 1978.

(19) Gutmann, V. *The Donor–Acceptor Approach to Molecular Interactions*; Plenum Press: New York, 1978.

(20) Smith, E. F.; Villar Garcia, I. J.; Briggs, D.; Licence, P. *Chem. Commun.* **2005**, 5633.

(21) Smith, E. F.; Rutten, F. J. M.; Villar-Garcia, I. J.; Briggs, D.; Licence, P. *Langmuir* **2006**, *22*, 9386.

(22) Lovelock, K. R. J.; Villar-Garcia, I. J.; Maier, F.; Steinrueck, H.-P.; Licence, P. *Chem. Rev.* **2010**, *110*, 5158.

(23) Villar-Garcia, I. J.; Smith, E. F.; Taylor, A. W.; Qiu, F.; Lovelock, K. R. J.; Jones, R. G.; Licence, P. *Phys. Chem. Chem. Phys.* **2011**, *13*, 2797.

(24) Shakeup, in terms of C 1s, is generally observed as an intense and defined component of up to 9% in intensity; as such, it is straightforward to include in peak-fitting models for quantification. Shakeup of N 1s, on the other hand, is not so easy to observe or quantify; it is generally a lot broader and less intense. Consequently, it is nontrivial to set thresholds and include as a regular component in quantitative peak-fitting models.

(25) Kratos Analytical, www.kratos.com, 2009.

(26) Sheldrick, G. M. *Acta Crystallogr., Sect. A* **2008**, *64*, 112.

(27) Dolomanov, O. V.; Bourhis, L. J.; Gildea, R. J.; Howard, J. A. K.; Puschmann, H. *J. Appl. Crystallogr.* **2009**, *42*, 339.

(28) Coles, S. J.; Gale, P. A. *Chem. Sci.* **2012**, *3*, 683.

(29) Ferraro, J. R. *Low-Frequency Vibrations of Inorganic and Coordination Compounds*; Plenum Press: New York, 1971.

(30) Illner, P.; Zahl, A.; Puchta, R.; van Eikema Hommes, N.; Wasserscheid, P.; van Eldik, R. *J. Organomet. Chem.* **2005**, *690*, 3567.

(31) Lungwitz, R.; Spange, S. *New J. Chem.* **2008**, *32*, 392.

(32) *IUPAC. Compendium of Chemical Terminology*, 2nd ed. (the 'Gold Book'); McNaught, A. D., Wilkinson, A., Eds.; Blackwell Scientific Publications: Oxford, U.K., 1997. Online version: http://goldbook.iupac.org, created by Nic, M.; Jirat, J.; Kosata, B.; updates by Jenkins, A.

(33) For example, see: Holbrey, J. D.; Reichert, W. M.; Nieuwenhuyzen, M.; Johnson, S.; Seddon, K. R.; Rogers, R. D. *Chem. Commun.* **2003**, 1636.

(34) Matsuzawa, H.; Nakai, R.; Ui, K.; Koura, N.; Ling, G. P. *Electrochemistry* **2005**, *73*, 715.

(35) Veith, M.; Godicke, B.; Huch, V. *Z. Anorg. Allg. Chem.* **1989**, *579*, 99.

(36) Zhong, C.; Sasaki, T.; Jimbo-Kobayashi, A.; Fujiwara, E.; Kobayashi, A.; Tada, M.; Iwasawa, Y. B. *Chem. Soc. Jpn.* **2007**, *80*, 2365.

(37) Yin, R. Z.; Yo, C. H. *Bull. Korean Chem. Soc.* **1998**, *19*, 947.

(38) Kapustinskii, A. F. *Q. Rev. Chem. Soc.* **1956**, *10* (3), 283.

(39) *Cambridge Structural Database (CSD)*, accessed 2011, Cambridge, U.K.